DOI: 10.61782/fa.2023.0398

forum acusticum 2023

TIME VARIANCE IN MEASURED ROOM IMPULSE RESPONSES

Karolina Prawda[1*] **Sebastian J. Schlecht**[1,2] **Vesa Välimäki**[1]

[1]Acoustics Lab, Dept. of Information and Communications Eng., Aalto University, Espoo, Finland
[2]Media Lab, Dept. of Art and Media, Aalto University, Espoo, Finland

ABSTRACT

Time variance is unavoidable in room impulse response (RIR) measurements, as the atmospheric conditions fluctuations and air movement prevent any room from being perfectly steady. However, the effect of such changes on RIRs has received little attention so far, although it is known to cause energy loss when RIRs are averaged to enhance their signal-to-noise ratio. In this work, we focus on the influence of spatio-temporal fluctuations in the speed of sound on RIR energy loss. We introduce a new approach to examining the relationship between time-variance-related energy loss of averaged RIRs and the decrease in their cross-correlation over time. We show that even when the measurements are compensated for the global changes in the speed of sound, the small fluctuations still contribute to the RIR dissimilarity. The results also indicate that the RIRs correlation decreases with the growing time separation between measurements. It shows that the short-term running cross-correlation is a good metric for estimating the time-variance-related energy loss in RIRs. The research presented in this work is a step towards more robust acoustic measurements and compensation of time-variance-related artifacts in measured signals.

Keywords: *acoustic measurements, acoustic signal processing, correlation, room impulse responses, time-varying systems.*

**Corresponding author*: karolina.prawda@aalto.fi.

1. INTRODUCTION

Time variance is the inherent contamination in room impulse response (RIR) measurements, occurring due to air movement and changes in the atmospheric conditions, such as temperature and humidity [1–8]. Those fluctuations influence the speed of sound during a measurement, which in consequence impacts the time-of-arrival (TOA) of reflections, causing each RIR to be time-stretched or time-compressed in comparison to the others in a series of repeated measurements [9–11].

The presence of transfer-function variation violates the assumption of a linear time-invariant system, leading to artifacts when noise-based excitation signals are used [1,4,6,12], and impairing sweep-based measurements, especially when using synchronous averaging [3,10,13,14]. This is critical when performing measurements in the ultrasound frequency range, such as scale-model measurements [15] as well as when multiple RIRs are compared, e.g., in scattering coefficient [16] and loudspeaker directivity measurements [17]. On the other hand, acoustic tomography takes advantage of time variance, using it to estimate the atmospheric conditions during a measurement [18–20].

The main technique used to estimate the amount of time variance in RIRs is using the short-term running cross-correlation of the measurements, and particularly studying the time lag of its maximal value [9–11]. Such an approach, however, is only applicable to considerable changes in the speed of sound that can cause substantial time-stretching in RIRs. In this work, we use the short-term running cross-correlation to estimate the transfer-function variation resulting from small fluctuations of speed of sound during a measurement. We propose a new approach to characterize the variation in TOA of reflections: by estimating the correlation loss relative to the expected correlation, i.e., correlation in time-invariant

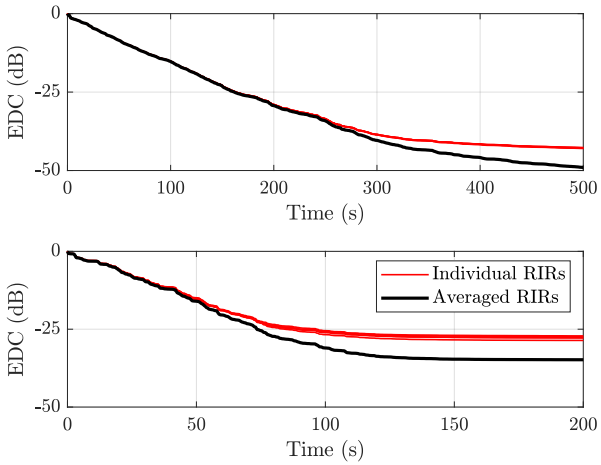

Figure 1: Examples of EDCs resulting from single RIR and five averaged RIRs for (top) broadband signal and (bottom) 19-kHz band.

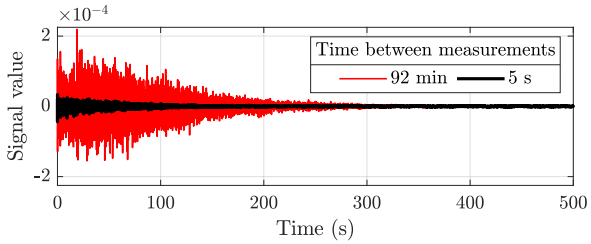

Figure 2: Difference between RIRs with different time separation between measurements.

conditions.

The paper is organized as follows. Section 2 describes the problems associated with time variance in RIR measurements and discusses the fluctuations in speed of sound. The methodology used to estimate the RIR correlation and to compensate for considerable time shifts is presented in Section 3. Section 4 describes the measurements used in this study and shows the results of energy and correlation comparison. The summary and conclusions are presented in Section 5.

2. PROBLEM FORMULATION

The fluctuations in the speed of sound may cause phase and TOA shifts in RIRs, visible either in a single RIR or when comparing consecutive measurements [6, 10]. This is particularly problematic when averaging is performed to increase the measurement's signal-to-noise ratio (SNR). In such a case, transfer-function variations lead to a well-known phenomenon of energy loss in the useful part of the averaged RIR compared to an RIR obtained from a single measurement, which is especially detrimental in high frequencies [11, 13].

An example of time-variance-induced RIR energy loss due to averaging is depicted in Fig. 1 on energy decay curves (EDCs) obtained from single RIRs and as a result of averaging five RIRs. In the top pane, a broadband signal is shown, presenting the loss of energy only in the late part of the signal, associated with improved SNR. In the bottom pane, EDCs for the 19-kHz band with 1-kHz bandwidth (±500 Hz from center frequency) show that in high frequencies the effect of averaging is more pronounced, causing RIR energy loss already in the early part of the signal. The difference between the averaged energy of five RIRs and the energy of five averaged RIRs reaches 1 dB within 50 ms from the direct sound.

In the literature, the change in the speed of sound is often assumed to be approximately homogeneous, meaning that the speed of sound is constant for the entire measurement period [1] or the changes occur slowly enough that the constant value is assumed anyway [11].

The effect of homogeneous atmospheric condition variations on the difference in speed of sound values between two RIRs is characterized by the time-stretching factor [1], which is independent of the initial measurement conditions and quantifies only the relative change in the speed of sound. The time-stretching factor is estimated based either on the known temperature [10] or short-term running cross-correlation [11]. Such solutions, however, have limitations, as it is well-known that temperature is only one of many components of time variance [1, 6, 9] and that the atmospheric conditions do not change in a regular manner, e.g., linearly or sinusoidally, but rather display small random fluctuations [21].

Two examples of differences between RIRs are shown in Fig. 2. The RIRs captured with 92 min elapsed in between them exhibit considerable differences, suggesting a big change in overall atmospheric conditions and, thus, in the speed of sound. However, the RIRs captured within 5 s from each other are also dissimilar according to the example of Fig. 2, starting from the direct sound, even though the changes in atmospheric conditions are very small, i.e., cannot be captured without highly sensitive specialized equipment. Therefore, a need for characterization and correction of quickly and randomly time-varying environments remains.

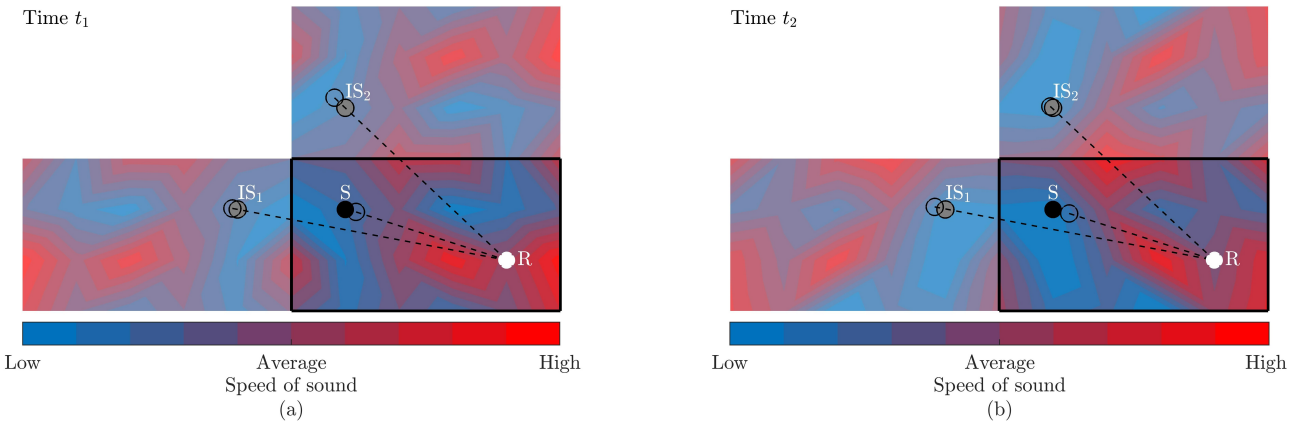

Figure 3: A 2-D view of a simulated room (black contour) with a sound source S (black dot), its images IS_1 and IS_2 (gray dots), and sound receiver R (white dot) at times (a) t_1 and (b) t_2. The spatial distribution of the speed of sound is marked with colors. The shift in distance between all sources (real and image) and the receiver is marked with transparent dots. The reflection paths are marked with dashed lines.

2.1 RIR variation

The atmospheric variation in the room is demonstrated in the changes of the speed of sound according to time and space, i.e., $c(t, \boldsymbol{x})$, where t is time and $\boldsymbol{x}$ is the Cartesian coordinate in space. The effective speed of sound is a combination of the scalar temperature-dependent Laplace speed of sound and the vector velocity field of the fluid [22]. In room acoustic simulations, $c(t, \boldsymbol{x})$ is usually chosen as time-invariant or even time- and space-invariant.

The variations of $c(t, \boldsymbol{x})$ alter the propagation time of reflections. This is illustrated in Fig. 3 on an example of changes to image-source positions in the image-source method (ISM). According to ISM, having room geometry with a sound source and a receiver, the image sources are created by reflecting the original source against the surfaces in the room geometry, and using those created images for further generating higher-order image sources [23]. The resulting image sources are marked in Fig. 3a and 3b with gray dots.

When atmospheric changes prompt fluctuations in the speed of sound, they are inhomogeneous in both time and space. In Fig. 3a and 3b, this is illustrated by the colored regions of shades of red and blue, marking the values of c above and below average, respectively, as well as by the configuration of those regions changing between both figures. The image-source positions are shifted, resulting in shorter or longer reflection paths between a given image source and a receiver, marked using transparent dots. The displacements of sound source positions in Fig. 3 are exaggerated for visual clarity, while the scale of the speed of sound c is for illustrative purposes only.

3. METHODOLOGY

In the following, we present the methodology used to assess the transfer-function variation in the measured RIRs. We discuss the RIR correlation and describe the method to compensate for time shifts caused by considerable changes in the speed of sound.

3.1 RIR correlation

Difference between RIRs presented in Fig. 2 indicate the level of time variance during measurements. However, subtracting two RIRs has the inherent disadvantage of being signal-value-dependent. The transfer-function variation affects the late part of an RIR to a greater extent since late reflections traverse through a varied environment for a longer period of time. However, RIR subtraction exhibits higher values in the beginning of the signal and lower towards the end of it.

In this study, we assess the amount of time variation in RIRs by examining their cross-correlation, as it is less affected by the gain of a reflection [24], and thus it is also immune to RIR changes caused by variation in atmospheric absorption of sound. Thus, we are able to focus on the differences in TOA of reflections.

We define a signal obtained in a measurement as

$$y_i(t) = h_i(t) + u_i(t), \tag{1}$$

where $h_i(t)$ is the RIR itself and $u_i(t)$ is the stationary background noise of the i^{th} measurement. Here, we treat the background noise as stationary since any non-stationary behavior is considered contamination which renders the measurement unfit for analysis [14, 25]. Thus, RIRs containing non-stationary noise were not used in this study.

The correlation between two signals, y_i and y_j, is as follows [14, 24, 26, 27]:

$$\begin{aligned}\rho_{y_i,y_j} &= \frac{\mathbb{E}[y_i\, y_j]}{\sqrt{\mathbb{E}[y_i^2]\,\mathbb{E}\left[y_j^2\right]}} \\ &= \frac{\mathbb{E}[(h_i + u_i)(h_j + u_j)]}{\sqrt{\mathbb{E}[(h_i + u_i)^2]\,\mathbb{E}[(h_j + u_j)^2]}},\end{aligned} \tag{2}$$

where $\mathbb{E}$ denotes the expected value.

We assume that the noise terms u_i and u_j, being random, are uncorrelated with the RIRs as well as with each other [14, 25], yielding $\mathbb{E}[u_i u_j] = 0$, $\mathbb{E}[h_j u_i] = 0$, and $\mathbb{E}[h_i u_j] = 0$, and transforming Eq. (2) into

$$\rho_{y_i,y_j} = \frac{\mathbb{E}[h_i h_j]}{\sqrt{(\mathbb{E}[h_i^2] + \mathbb{E}[u_i^2])(\mathbb{E}\left[h_j^2\right] + \mathbb{E}\left[u_j^2\right])}}. \tag{3}$$

In time-invariant conditions, the RIRs are considered identical, i.e., $h_i = h_j$. This makes their energies equal, too, $\mathbb{E}\left[h_i^2\right] = \mathbb{E}\left[h_j^2\right]$. A similar relation holds for the noise energies under the assumption of stationary background noise, $\mathbb{E}\left[u_i^2\right] = \mathbb{E}\left[u_j^2\right]$ [14].

When the conditions of time-invariance and stationary background noise are fulfilled, the correlation between two RIR measurements can be expressed by means of SNR:

$$\widehat{\rho}_{y_i,y_j} = \frac{\mathbb{E}\left[h^2\right]}{\mathbb{E}[h^2] + \mathbb{E}[u^2]} = \frac{\mathrm{SNR}}{1 + \mathrm{SNR}}, \tag{4}$$

where the SNR is defined as:

$$\mathrm{SNR} = \frac{\mathbb{E}\left[h^2\right]}{\mathbb{E}[u^2]}. \tag{5}$$

3.2 Short-term running cross-correlation

In the present work, we calculate the correlations ρ_{y_i,y_j} and $\widehat{\rho}_{y_i,y_j}$ using the short-term running cross-correlation.

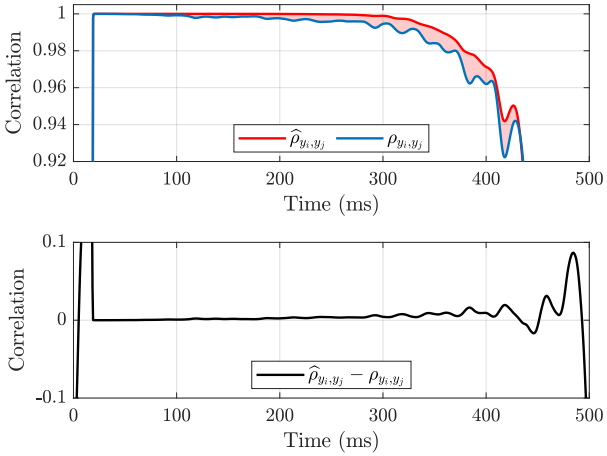

Figure 4: (Top) Comparison between the measured correlation $\rho_{y_i,y_j}(t')$ and the correlation $\widehat{\rho}_{y_i,y_j}(t')$ of an ideal time-invariant system only affected by background noise. The difference caused by time variance is indicated in the red-shaded area. (Bottom) The difference between the expected and measured correlation grows over time.

It is an established method in estimating the effect of time variance on RIRs, as it captures the associated subtle and quick changes in the signal [9,11]. First, we define a short-term version of y_i at time t as

$$y_i^{t'}(t) = w(t - t')\, y_i(t), \tag{6}$$

where w is a Hanning window used here to smooth the cross-correlation curves, and t' is the window center time. We define $y_j^{t'}$ and $h^{t'}$ equivalently. We then apply Eq. (6) to Eq. (2), obtaining

$$\rho_{y_i,y_j}(t') = \frac{\mathbb{E}\left[y_i^{t'}\, y_j^{t'}\right]}{\sqrt{\mathbb{E}\left[(y_i^{t'})^2\right]\,\mathbb{E}\left[(y_j^{t'})^2\right]}}. \tag{7}$$

Similar modifications are made to Eq. (4):

$$\widehat{\rho}_{y_i,y_j}(t') = \frac{\mathbb{E}\left[(h^{t'})^2\right]}{\mathbb{E}[(h^{t'})^2] + \mathbb{E}[u^2]} \tag{8}$$

defining the short-term running cross-correlation in time-invariant conditions. In Eq. (8) only the parts regarding the RIR itself are calculated in the short windows, as short-term noise energy is hard to separate from the RIR [25, 28]. Thus, $\mathbb{E}\left[u^2\right]$ is computed as one number for

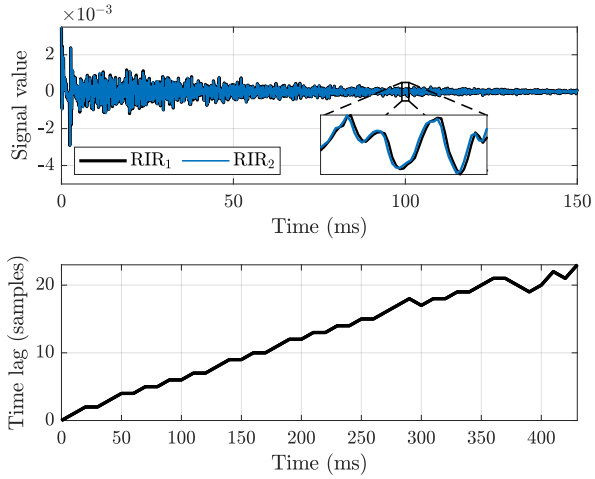

Figure 5: (Top) Two RIRs with a 92-min separation between measurements and a zoom into a 1 ms signal segment, showing a minor time shift. (Bottom) Time lag of the short-term running cross-correlation grows over time.

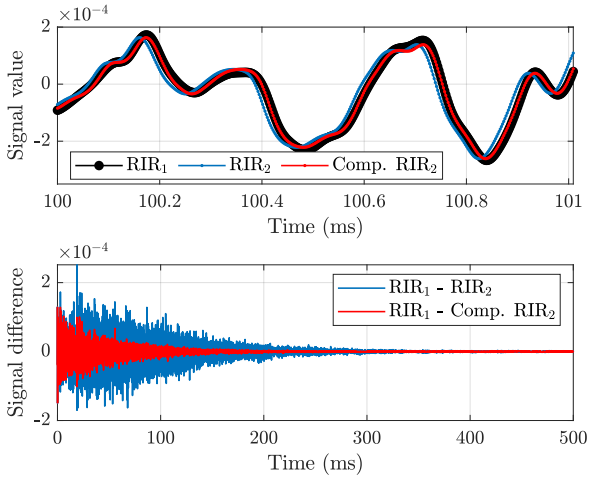

Figure 6: (Top) 1-ms snippet of the upsampled initial RIRs and time-shifted version of the second RIR (*cf.* top pane of Fig. 5). (Bottom) Differences between the reference RIR and the second RIR, and the compensated second RIR, showing a reduction.

the entire measurement, using the part of the signal where the RIR has already decayed below the noise floor level.

Figure 4 shows an example of the progression of $\rho_{y_i,y_j}(t')$ and $\widehat{\rho}_{y_i,y_j}(t')$ over time. The values of expected correlation $\widehat{\rho}_{y_i,y_j}(t')$ are stable until the RIRs have decayed enough that the background noise causes a sudden drop in correlation values. The measured correlation $\rho_{y_i,y_j}(t')$ is consistently lower than the expected value, with the difference growing over time. This indicates that the time variance has a detrimental effect on the RIR correlation.

3.3 Time-shift compensation

This work focuses on small fluctuations in speed of sound due to the inhomogeneity of atmospheric conditions within the measurement time. However, given sufficient time separation between measurements, a global shift in c is observed as well, leading to a considerable macro shift in reflections TOA. It is illustrated in the top pane of Fig. 5, where the time separation between two RIR measurements was 92 minutes. Zooming into the later part of the signals reveals a one-sample ($\sim$ 0.02 ms for sampling rate of 44.1 kHz) shift in the TOA of the second RIR.

Here, we compensate for the time shift created by change of the average speed of sound during a measurement. We use the method proposed by Postma and Katz [11], in which the RIRs are first upsampled by the factor of 10. Then, their short-term running cross-correlation is computed, and the time lag of its maximal value is obtained. Over time, the lag increases linearly, as shown in the bottom pane Fig. 5, indicating the change in temperature between measurements. The slope m of the lag is estimated with the least-squares optimization method, and the resampling by the factor of $10\,f_\mathrm{s}/(10\,f_\mathrm{s}+m)$ is applied to the RIRs.

The top pane of Fig. 6 presents a 1-ms snippet of 10-times upsampled RIRs. The time shift introduced by the changes in the speed of sound c is successfully removed. It significantly reduces the difference between the two RIRs, shown in the bottom pane of Fig. 6. However, time-shift-compensated RIRs retain a degree of dissimilarity, indicating the presence of remaining time variance.

4. RESULTS

This section describes the measurements used for gathering RIRs analyzed in the present study. It also compares the energy loss between averaged RIRs to the RIR cross-correlation.

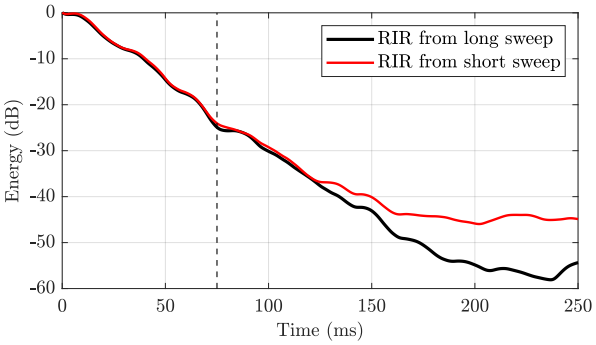

Figure 7: The energy of RIRs obtained from measurements using a 58-s-long and a 3-s-long sweep. The energy of the long sweep RIR starts to be visibly lower than energy of short sweep RIR around 75 ms, which is marked with the dashed line.

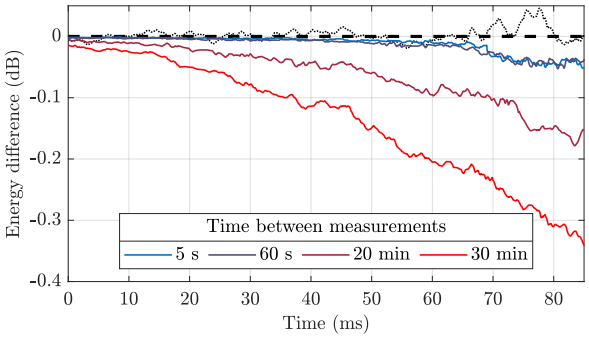

Figure 8: Energy loss in 19-kHz band for two averaged RIRs with different time separation. (——) symbolizes the measured energy differences between averaged RIRs and a single RIR, whilst (· · ·) shows an example of the energy difference of two single RIRs. (- - -) marks the 0-dB line.

4.1 Measurement setup

The measurements were conducted in *Arni*, a variable acoustics laboratory at Aalto University in Espoo, Finland. It is a shoebox room with dimensions 8.9 m × 6.3 m × 3.6 m (length, width, and height, respectively), which has 55 variable acoustic panels located on the walls and ceiling, allowing for changing the sound absorption configuration in the room. For the purpose of this study, the measurements were conducted in the most absorptive setting (all panels closed) [29, 30]. The equipment used in the measurements was: 01dB LS01 omnidirectional loudspeaker, a G.R.A.S. 1/2-inch diffuse-field microphone of type 40AG, a G.R.A.S. power module of type 12AG, and a MOTU UltraLite mk3 Audio Interface.

The measurements used 3-s-long exponentially-swept sines (ESSs) as excitation signals and 2 s of silence between consecutive ESSs to allow the sound to decay completely. The excited frequencies spanned from 20 Hz to 20 kHz, and the SNR reached 45 dB.

4.2 Energy loss and correlation

To separate the effect of energy loss due to time variance and the SNR gain, an additional measurement of a 58-s-long sweep was performed using the same measurement setup as described in Sec. 4.1. Fig. 7 depicts the energy of both RIRs. The decrease in the energy of long sweep RIR is visible from around 75 ms, as marked with the dashed line. It indicates that from this point on, the noise becomes more dominant in the RIR, suggesting that energy losses due to averaging may come from the enhanced SNR additionally to time-variance-related losses. Thus, in the further analysis, we focus only on the first 75 ms of the signals.

The RIR energy loss was studied by comparing the averaged energy of single RIRs to energy of two averaged RIRs, following

$$\Delta\,\mathbb{E} = \mathbb{E}\left[\frac{y_i + y_j}{2}\right] - \frac{\mathbb{E}[y_i] + \mathbb{E}[y_j]}{2}. \qquad (9)$$

The analysis was conducted for bandpassed signals in 19-kHz band with bandwidth of 1 kHz (±500 Hz from the center frequency) as the losses are most visible in high frequencies (*cf.* Fig. 1). All RIRs were time-shift compensated before the calculations (*cf.* Sec. 3.3).

The results of energy difference comparison are presented in Fig. 8 for time separations of 5 s, 60 s, 20 min, and 30 min. To decrease the noisiness of the curves, they were obtained by averaging energy differences for 50 pairs of RIRs for each time separation. Additionally, the dotted line presents the energy difference between two single RIRs as a reference.

Figure 8 shows that averaging of the RIRs always leads to RIR energy loss in high frequencies, even when the measurements are performed shortly after one another, such as with 5 s of time separation. The loss increases over the duration of RIRs and proportionally to the growing time separation between measurements.

Figure 9 shows the short-term running cross-

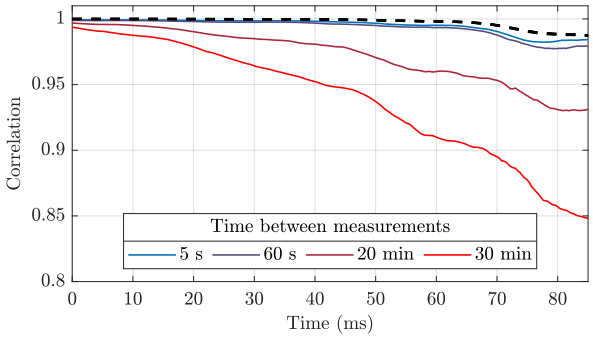

Figure 9: Measured correlation ρ_{y_i,y_j} between two averaged RIRs (——) and their expected correlation $\widehat{\rho}_{y_i,y_j}$ (- - -).

correlation of RIRs ρ_{y_i,y_j} computed based on Eq. (7). The correlation expected in time-invariant conditions calculated according to Eq. (8) is marked with dashed lines. The correlation is calculated for the same pairs of RIRs that were used to obtain results in Fig. 8, and the curves in Fig. 9 are the outcome of averaging 50 trials for each time separation.

The results depicted in Fig. 9 show that the correlation between two RIRs never achieves the time-invariant expected values, even though ρ_{y_i,y_j} is very close to $\widehat{\rho}_{y_i,y_j}$ in the first 20–30 ms of the signal. Over the RIR duration, the correlation decrease becomes more pronounced, especially for large time separations. The $\widehat{\rho}_{y_i,y_j}$ curves overlap for all analyzed RIR pairs, proving that the change in background noise does not influence the correlation drop.

The similarities between Figs. 8 and 9 suggest that there is a link between the RIR correlation and time-variance-induced RIR energy loss. The shape and order of curves correspond to each other in both figures. This indicates that the correlation is a good measure of the effect of time variance on RIRs and that the energy loss due to RIR averaging can be predicted using such a metric.

5. CONCLUSIONS

In the present work, we investigate the impact of time variance on measured RIRs and the energy loss of averaged RIRs in particular. We first show the extent of the problem by displaying the detrimental effect of transfer-function variation on averaged RIRs energy, most prominent in high frequencies. As this study focuses on time variance caused by small fluctuations in the speed of sound during the measurement, the global shifts in values of the speed of sound are compensated for.

We assess the extent of time variance in RIRs by examining the energy loss in averaged RIRs compared to the energy of single RIRs. We also show that time variance affects the correlation of a pair of RIRs. We present both metrics for RIRs with different time elapsed between measurements, starting from 5 s and ending with 30 min.

The results show a visible connection between the RIR correlation and time-variance-induced energy loss. Both metrics exhibit a similar behavior over the duration of RIRs and a growing time separation. It indicates that short-term running cross-correlation is a good indicator of the time variance in RIR measurements.

Future work may include developing a model to predict and compensate for the energy loss based on RIR correlation. The insights presented here are a step towards more robust and reliable acoustic measurements.

6. ACKNOWLEDGMENTS

This work belongs to the activities of the Nordic Sound and Music Computing Network (NordForsk project number 86892).

7. REFERENCES

[1] P. Svensson and J. L. Nielsen, “Errors in MLS measurements caused by time variance in acoustic systems,” *J. Audio Eng. Soc.*, vol. 47, no. 11, pp. 907–927, 1999.

[2] S. Müller and P. Massarani, “Transfer-function measurement with sweeps,” *J. Audio Eng. Soc.*, vol. 49, no. 6, pp. 443–471, 2001.

[3] M. Guski, *Influences of External Error Sources on Measurements of Room Acoustic Parameters*. PhD thesis, RWTH Aachen University, Germany, 2015.

[4] T. Niederdränk, “Maximum length sequences in non-destructive material testing: application of piezoelectric transducers and effects of time variances,” *Ultrasonics*, vol. 35, no. 3, pp. 195–203, 1997.

[5] F. Georgiou, M. Hornikx, and A. Kohlrausch, “Auralization of a car pass-by inside an urban canyon using measured impulse responses,” *Appl. Acoust.*, vol. 183, 2021. paper no. 108291.

[6] M. Vorländer and M. Kob, “Practical aspects of MLS measurements in building acoustics,” *Appl. Acoust.*, vol. 52, no. 3-4, pp. 239–258, 1997.

[7] V. E. Ostashev and D. K. Wilson, *Acoustics in Moving Inhomogeneous Media*. CRC Press, 2015.

[8] G. W. Elko, E. Diethorn, and T. Gänsler, "Room impulse response variation due to thermal fluctuation and its impact on acoustic echo cancellation," in *Proc. Int. Workshop on Acoustic Echo and Noise Control*, 2003.

[9] F. Satoh, "Acceptable temperature changes during synchronous averaging for reverberation time measuring by swept-sine method," in *Proc. 19th Int. Congr. Acoust. (ICA)*, (Madrid, Spain), pp. 1–6, Sept. 2007.

[10] X. Wang, *Model based signal enhancement for impulse response measurement*. Doctoral dissertation, RWTH Aachen University, Aachen, Germany, 2013.

[11] B. N. J. Postma and B. F. G. Katz, "Correction method for averaging slowly time-variant room impulse response measurements," *J. Acoust. Soc. Am.*, vol. 140, no. 1, pp. EL38–EL43, 2016.

[12] K. Mori and Y. Kaneda, "Robustness of pure white pseudonoise signal to temporal fluctuation in impulse response measurement," *Acoust. Sci. Technol.*, vol. 38, no. 3, pp. 168–170, 2017.

[13] A. Farina, "Advancements in impulse response measurements by sine sweeps," in *Proc. AES 122nd Conv.*, (Vienna, Austria), May 2007.

[14] K. Prawda, S. J. Schlecht, and V. Välimäki, "Robust selection of clean swept-sine measurements in non-stationary noise," *J. Acoust. Soc. Am.*, vol. 151, no. 3, pp. 2117–2126, 2022.

[15] K. Baruch, A. Majchrzak, B. Przysucha, A. Szelag, and T. Kamisiński, "The effect of changes in atmospheric conditions on the measured sound absorption coefficients of materials for scale model tests," *Appl. Acoust.*, vol. 141, pp. 250–260, 2018.

[16] L. Shtrepi, A. Astolfi, G. D'Antonio, G. Vannelli, G. Barbato, S. Mauro, and A. Prato, "Accuracy of the random-incidence scattering coefficient measurement," *Appl. Acoust.*, vol. 106, pp. 23–35, 2016.

[17] T. Knüttel, I. B. Witew, and M. Vorländer, "Influence of "omnidirectional" loudspeaker directivity on measured room impulse responses," *J. Acoust. Soc. Am.*, vol. 134, no. 5, pp. 3654–3662, 2013.

[18] M. Bleisteiner, M. Barth, and A. Raabe, "Tomographic reconstruction of indoor spatial temperature distributions using room impulse responses," *Meas. Sci. Technol.*, vol. 27, Feb. 2016. paper no. 035306.

[19] N. S. Dokhanchi, J. Arnold, A. Vogel, and C. Voelker, "Measurement of indoor air temperature distribution using acoustic travel-time tomography: Optimization of transducers location and sound-ray coverage of the room," *Measurement*, vol. 164, 2020. paper no. 107934.

[20] L. Tronchin, "Variability of room acoustic parameters with thermo-hygrometric conditions," *Appl. Acoust.*, vol. 177, 2021. paper no. 107933.

[21] A. Melikov, U. Krüger, G. Zhou, T. Madsen, and G. Langkilde, "Air temperature fluctuations in rooms," *Build. Environ.*, vol. 32, no. 2, pp. 101–114, 1997.

[22] P. Holstein, A. Raabe, R. Müller, M. Barth, D. Mackenzie, and E. Starke, "Acoustic tomography on the basis of travel-time measurement," *Meas. Sci. Technol.*, vol. 15, no. 7, p. 1420, 2004.

[23] L. Savioja and U. P. Svensson, "Overview of geometrical room acoustic modeling techniques," *J. Acoust. Soc. Am.*, vol. 138, no. 2, pp. 708–730, 2015.

[24] M. Borga, "Canonical correlation: A tutorial," *Online tutorial http://people.imt.liu.se/magnus/cca*, vol. 4, no. 5, 2001.

[25] K. Prawda, S. J. Schlecht, and V. Välimäki, "Short-term rule of two: Localizing non-stationary noise events in swept-sine measurements," in *Proc. AES 154th Conv.*, (Espoo, Finland), May 2023.

[26] K. Prawda, S. J. Schlecht, and V. Välimäki, "Multichannel interleaved velvet noise," in *Proc. Int. Conf. Digital Audio Effects (DAFx)*, (Vienna, Austria), pp. 208–215, Sept. 2022.

[27] J. Benesty, J. Chen, and Y. Huang, "On the importance of the Pearson correlation coefficient in noise reduction," *IEEE Trans. Audio Speech Lang. Process.*, vol. 16, pp. 757–765, May 2008.

[28] M. Guski and M. Vorländer, "Impulsive noise detection in sweep measurements," *Acta Acust. united Ac.*, vol. 101, no. 4, pp. 723–730, 2015.

[29] K. Prawda, S. J. Schlecht, and V. Välimäki, "Calibrating the Sabine and Eyring formulas," *J. Acoust. Soc. Am.*, vol. 152, no. 2, pp. 1158–1169, 2022.

[30] K. Prawda, S. J. Schlecht, and V. Välimäki, "Evaluation of reverberation time models with variable acoustics," in *Proc. 17th SMC Conf.*, (Torino, Italy), pp. 145–152, June 2020.